Airspeed Control of Electric Airplane Based on 2-Quadrant Thrust Control and Verification with Towing Test Using Electric Vehicle

Kenichiro Takahashi, Hiroshi Fujimoto, and Yoichi Hori
Graduate School of Frontier Sciences,
The University of Tokyo
5-1-5 Kashiwanoha, Kashiwa-shi, Chiba, 277-8561 Japan
Phone and Fax: +81-4-7136-3881

Hiroshi Kobayashi and Akira Nishizawa
Institute of Aeronautical Technology
Japan Aerospace Exploration Agency
6-13-1 Osawa, Chofu-shi, Tokyo 181-0015
Telephone: +81-50-3362-4458

***Abstract*—Electrical airplanes (EAs) have become practical in the recent years. Considering the increase of demand on smaller aircraft and the attention to environmental issues, the demand on small EAs is expected to grow in the coming decade. However, the accident rate of small aircrafts is higher than that of larger aircrafts, so ensuring higher safety of EA is very urgent. Modeling and thrust control and of EAs have been proposed previously by the authors' research group. However, this model and control method cannot express the model and control the thrust when the propeller revolution speed is near and below zero. In this paper, the new thrust control method based on new EA propeller plant is proposed. This method is necessary for future design of airspeed control method, which can be expected to improve the safety of EA. The effectiveness of the proposed method is verified through simulations and experiments.**

I. Introduction

A. Background

Recently, light airplanes such as light general aviation is increasing rapidly [1]. However, business aircraft have a fatal accident rate approximately 10 times higher than that of large commercial jets [2], and improvement of safety is required. A great number of the accidents are caused by weather change, regardless of the size of the airplane [3], [4], and rising the safety verses weather is urgent.

Electric airplanes have become widely noticed for environmental reasons [5]. Furthermore, electric airplanes have not only environmental advantages, but electric motors have characteristics as listed below.

- The torque response of electric motors is 100-500 times faster than that of engines.
- The output torque can be measured accurately from the motor current.
- Dispersed placement and independent control can be done easily, and the flexibility of the plane design and the degree of freedom of control is higher.
- Physical energy can be regenerated to electric energy.

Many researches have been carried out with electric vehicles (EVs) using these merits [6], [7].

Technological exchange between the automotive and aviation industry have been active ever since the Wright brothers took flight [8]. If the airplane becomes motorized, the motion control theories highly developed in the automotive industry can be expected to be adapted to airplanes [9].

B. Objective

Including EAs, present airplanes are designed to give higher stability and controllability. For example, the wings of an airplane is swept back and has a dihedral angle, and the tail assemblies are designed large. However, these structures increase drag, or request higher strength which make the airplane heavier. One solution is to compensate the stability with control, but conventional airplanes only have three main control surfaces, and this is not enough to control the 6 degree of freedom the airplane has. The thrust is another factor that may be controlled, and thrust control method of engines have been researched [10], but the controlling of output torque is difficult, and the thrust control system is complex and the response speed is not high.

On the other hand, electric airplanes' thrust can be controlled easily due to the characteristics listed above. By developing high response accurate thrust control using electric motor, high performance airspeed control can be developed. Furthermore, by harmoniously controlling dispersed placed motor, completely new control methods that could not be adopted to conventional airplanes can be conceivable.

Therefore, modeling and thrust control method of electric airplane has been studied by the authors' research group [11]. However, this modeling uses a variable which has revolution speed on its denominator. Revolution speed must fall below zero in order to generate negative thrust under a certain point. This restricts the model to be used when the propeller revolution speed is near zero. Moreover, the plant can not be expressed continuously by revolution speed when revolution speed crosses zero.

This paper will propose a 2-quadrant thrust control method, airspeed control of EA, and novel towing test method using EA. Here, 2-quadrant is defined by the combination of propeller thrust and airspeed, not motor torque and revolution speed. The proposed methods will be verified by simulations.

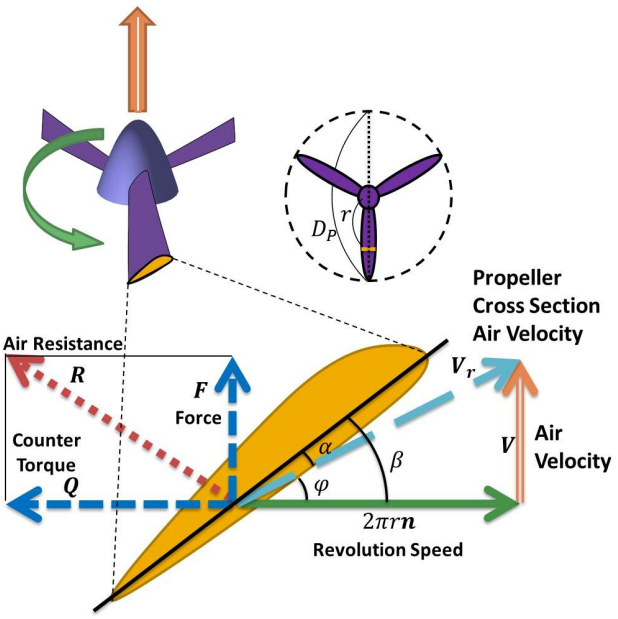

Fig. 1. Physics of propeller cross section [12]

II. Modeling of Single Motor Electric Airplane

In this section, the single motor electric airplane will be modeled. This model is based on the model previously proposed in cite [11]. First, the physics that determine thrust and counter torque will be explained. Than, the equation of motion is derived. Finally, the equations will be arranged into a block diagram as a model of the propeller airplane.

Fig. 1 is the cross section of a propeller blade at distance r from the hub. While flying, the propeller cross section moves as a composition of rotation and advance motion. Therefore, the cross section moves as a spiral. Assume the airspeed to be parallel with the axis of the propeller. Airspeed is the relative velocity between the air and airplane. When n is propeller revolution speed and $\boldsymbol{V}$ is the airspeed vector, the propeller cross section's airspeed $\boldsymbol{V}_r$ is the sum of revolution speed vector and airspeed vector as

$$\boldsymbol{V}_r = 2\pi r\boldsymbol{n} + \boldsymbol{V} \tag{1}$$

where $\boldsymbol{n}$ is a vector with a length of n with a rotation direction. Therefore, air stream attacks the propeller cross section as vector $-\boldsymbol{V}_r$.

The cross section takes a counter force vector $\boldsymbol{R}$. $\boldsymbol{R}$ can be resolved into the direction of the motion of the airplane vector $\boldsymbol{F}$, and the direction of propeller revolution vector $\boldsymbol{q}$.

$$\boldsymbol{R} = \boldsymbol{F} + \boldsymbol{Q}/r \tag{2}$$

The propeller cross section is a airfoil, so counter force $\boldsymbol{R}$ depend on the angle of attack α. Generally, it is known that the resolved force parallel to the air stream is increasing convex function of alpha, and the resolved force perpendicular to the air stream is a function with a peak.

The angle between vector $\boldsymbol{V}_r$ and the surface of propeller revolution φ is defined as angle of advance. The angle of attack α can be represented as

$$\begin{aligned} \alpha &= \beta - \varphi & (3)\\ &= \beta - \arctan\left\{\frac{1}{2\pi r}\cdot\frac{V}{n}\right\} & (4)\end{aligned}$$

where β is the angle between the chord of blade of the propeller cross section and the revolution surface, $V = |\boldsymbol{V}|$, and $n = |\boldsymbol{n}|$. As shown in Eq. (4), the angle of attack α is a function of V/n. When inverse advance ratio y is defined as a dimensionless equation as Eq. (5), $\boldsymbol{F}$ and $\boldsymbol{Q}$ is a function of y.

$$y = \frac{nD_p}{V} \tag{5}$$

From the above, when propeller counter torque $Q = |\boldsymbol{Q}|$ and thrust $F = |\boldsymbol{F}|$ is represented as Eq. (6) and Eq. (7), dimensionless coefficient Q_C and F_C is a nonlinear function of J.

$$\begin{aligned} Q &= Q_C\rho V^2 D_p^3 & (6)\\ F &= F_C\rho V^2 D_p^2 & (7)\end{aligned}$$

Here, ρ is air density.

A. Equation of Motion of Propeller and Body

Here, only the direction of movement is considered, and is assumed that airspeed and thrust change does not affect the attitude of the airplane. The propeller's equation of revolutionary motion and body's equation of translational motion is expressed as

$$\begin{aligned} J_\omega\dot{\omega} &= T - Q, \qquad \omega = 2\pi n & (8)\\ M\dot{V}_E &= F - D & (9)\end{aligned}$$

where J_ω is the inertia moment of the propeller, ω is the angular velocity of the propeller, T is motor torque, M is plane mass, V_E is the relative speed between the ground and air, or ground speed, and D is drag.

By using drag coefficient C_D, drag D can be expressed as

$$C_D = \frac{D}{\frac{1}{2}\rho V^2 S} \tag{10}$$

where S is wing area.

The relation ship between airspeed V, groundspeed V_E, and tailwind U is expressed as

$$V = V_E - U. \tag{11}$$

From Eq. (8)–(11), the model of a single propeller airplane can be expressed as Fig. 2.

III. Designing of Thrust Control of Single Propeller Electric Airplane

In this section, new 2-quadrant thrust control method is proposed. The thrust controller has a counter torque observer and a revolution speed controller previously proposed in cite [11]. The revolution speed controller is shown in Fig. 3.

The transfer function from n^* to n is express as Eq. (12), and is defined G_{nn^*}.

$$\frac{n}{n^*} = \frac{C_1 P_{1n}}{s + C_1 P_{1n}} = \frac{\omega_1}{s + \omega_1} = G_{nn^*} \tag{12}$$

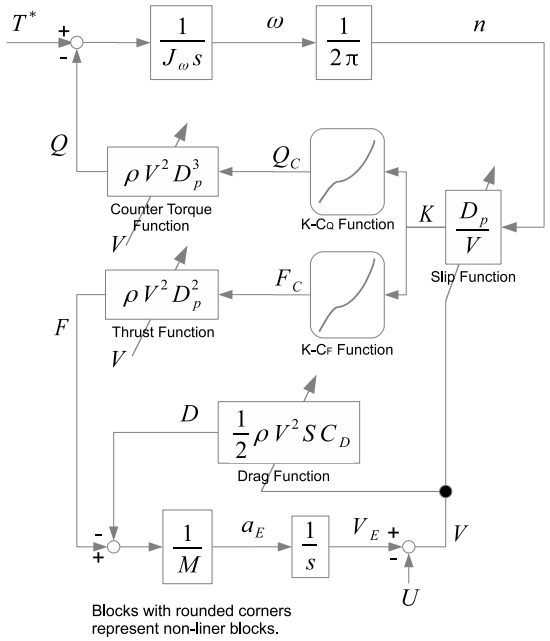

Fig. 2. Propeller model

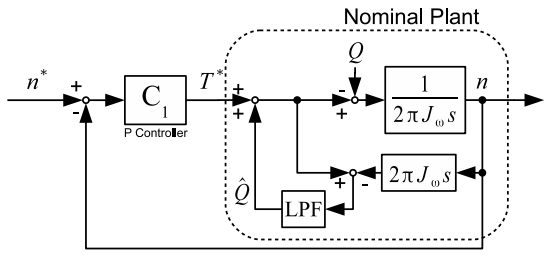

Fig. 3. Revolution speed controller

A. Designing of Thrust Controller

In this part, the thrust controller is designed. The thrust controller is designed as a two-degree-of-freedom control as shown in Fig. 4.

C_F can be quadratically approximated. From Eq. (7), thrust F can be rewritten using coefficients a_{CF}, b_{CF}, and c_{CF} as

$$\begin{aligned} F &= \left(a_{\mathrm{CF}}J^2 + b_{\mathrm{CF}}J + c_{\mathrm{CF}}\right)\rho n^2 D_p^4 \\ &= c_{\mathrm{CF}}\rho D_p^4 n^2 + b_{\mathrm{CF}}\rho D_p^3 V n + a_{\mathrm{CF}}\rho D_p^2 V^2. \end{aligned} \quad (13)$$

Define function f as a function between revolution speed n and F as

$$F = f(n). \quad (14)$$

However, Thrust F is also a function of airspeed V, so V varies the non liner function f.

Feed forward controller C_3 is designed as follows. Thrust F is a function of n^* as

$$F = f(G_{nn^*} \cdot n^*). \quad (15)$$

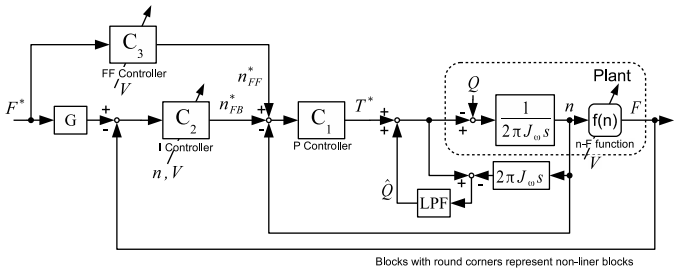

Fig. 4. Thrust controller

Therefore,

$$\begin{aligned} n^* &= G_{nn^*}^{-1} \cdot f^{-1}(F) \\ &= \frac{s+\omega_1}{\omega_1} f^{-1}(F). \end{aligned} \quad (16)$$

Eq. (16) is non-proper, so feed forward controller C_2 is designed using reference model $G_0(s)$.

$$G_0(s) := \frac{\omega_g}{s+\omega_g} \quad (17)$$

$$n^* = f^{-1}(F) \cdot G_{nn^*}^{-1} \cdot G_0(s) \quad (18)$$

Here, ω_g is the pole of the reference model. Because $f^{-1}(F)$ varies by V and is non liner, feed forward controller C_2 is a non liner variable controller as shown in Eq. (18).

Next, feedback controller C_3 is designed as follows. Feedback reference F_{FB}^* is created by multiplying reference model $G_0(s)$ to thrust reference F^* as $F_{FB}^* = G_0(s)F^*$. By using Taylor series at operating point $n = n_0$, $f(n)$ can be approximated to its first order. When the first order coefficient is $a_F(n_0, V)$ and the intercept is $b_F(n_0, V)$, Eq. (19) is obtained.

$$F \approx a_F n + b_F \quad (19)$$

The revolution speed controller is assumed to be fast enough so $n = n^*$. The feed back controller uses the difference of the reference and output, so when b_F is regarded as a constant, Eq. (20) can be obtained as plant P_2.

$$P_2 := \frac{\Delta F}{\Delta n^*} = \frac{\Delta F}{\Delta n} = a_F \quad (20)$$

Thrust control uses integral controller, and the gain is decided so the pole is placed at $-\omega_2$ while the plant is assumed to be P_2. Here, a_F is a function of n_0 and V, so thrust feedback controller C_3 is a variable controller where n_0 is substituted by n successively.

IV. Comparison of Thrust Controllers through Simulations

Thrust control method proposed in section III is verified by two simulations. The plants used for the simulations only consider the propeller's physics, and the body's dynamics were not considered. That is, the propeller was considered to operate at a given airspeed.

The poles of each controller were placed as following; the revolution speed controller at $\omega_0 = 0.4$ rad/s and $\omega_1 = 100$ rad/s, the pole of the thrust controller at $\omega_2 = 50$ rad/s, and the pole of the reference model at $\omega_g = 50$ rad/s.

TABLE I. PARAMETERS OF PROPELLER

Propeller Diameter D_p	178 mm
Propeller Inertia J_ω	1.06×10^{-5} kg·m
Air Density ρ	1.23 kg/m^3

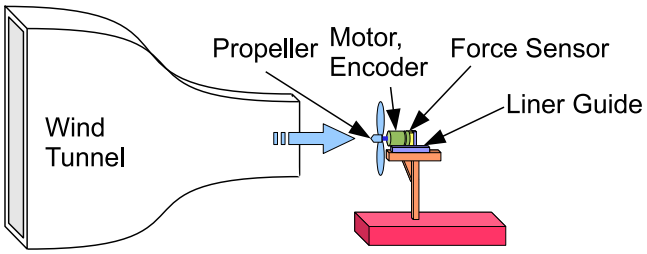

Fig. 5. Schematic Diagram of Experimental Unit

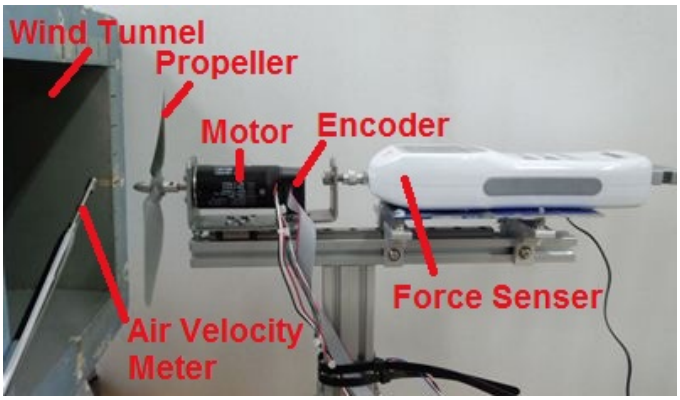

Fig. 6. Picture of Experimental Unit

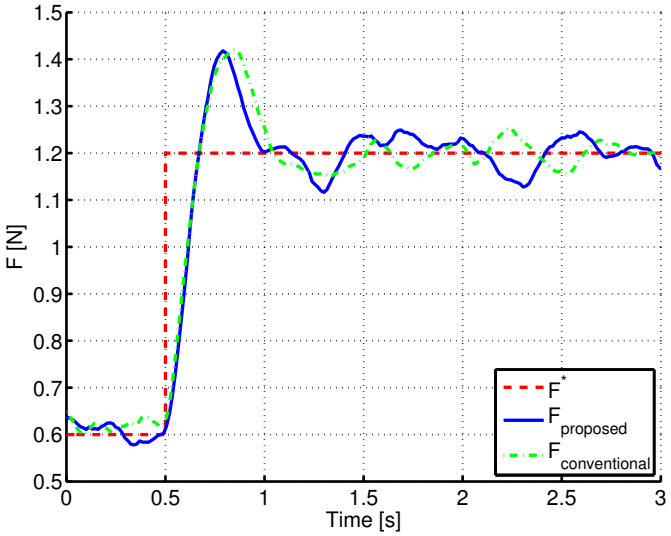

Fig. 7. Step Responce

V. COMPARISON OF THRUST CONTROLLERS THROUGH EXPERIMENT

The effectiveness of the proposed method was verified though two experiments.

A. Experimental Setup

In this part, the experimental unit made for this research will be explained. The experimental unit is shown in Fig. 5 and (6). The unit consists of liner guide, force sensor, motor mount, motor, encoder, propeller, anemometer, and wind tunnel.

The propeller is connected to the motor, and the thrust is measured by the force sensor. The propeller is set at 5 cm from the opening of the wind tunnel, so that the axis of the propeller is parallel with the wind. The anemometer is fixed at the opening of the wind tunnel. The size of the opening of the wind tunnel is 200 mm $\times$ 200 mm.

Because the anemometer is set in front of the propeller, even when the wind tunnel is set at same speed, the measured wind speed is enlarged. The speed of air in front of the propeller is also larger than the airspeed of a real airplane. This experimental unit does not have a wind tunnel large enough compared to the propeller, the airspeed was assumed that it is the measured value when the power given to the propeller was zero.

The pseudo-differentiation of the angle measured by the encoder was used acquire revolution speed.

The poles of each controller were placed as following; the revolution speed controller at $\omega_0 = 0.4$ rad/s and $\omega_1 = 100$ rad/s, the pole of the thrust controller at $\omega_2 = 50$ rad/s, and the pole of the reference model at $\omega_g = 50$ rad/s.

The experimental model uses the parameter of APC 7x6 SF model propeller. The parameters are as listed in Table I. The parameters are shown in Table I.

B. Step Response of Thrust

Step response experiment was carried out to the thrust controller. The airspeed was fixed, and a step reference was given. The airspeed V was set at $V = 7$ m/s, and the experiment started at a steady state of thrust at $F = 0.60$ N. At $t = 0.5$ s, thrust reference changed from 0.60 N to 1.20 N.

The experiment results are shown in Fig. 8. The conventional and proposed methods have very similar responses.

C. Negative Step Response of Thrust

Next a negative thrust reference was given to the thrust controllers. The airspeed V was set at $V = 7$ m/s, and the experiment started at a steady state of thrust at $F = 0.80$ N. At $t = 0.5$ s, thrust reference changed from 0.80 N to -0.80 N.

The experiment results are shown in Fig. 8. The conventional method was not able to follow the thrust reference at negative thrust. The experimental setup had torque and revolution speed limiters, but without them, the thrust would have diverged. The proposed method was able to follow the thrust reference even at negative reference.

VI. AIRSPEED CONTROL METHOD

In this section, airspeed control method using force control method proposed in section III will be proposed. Here the

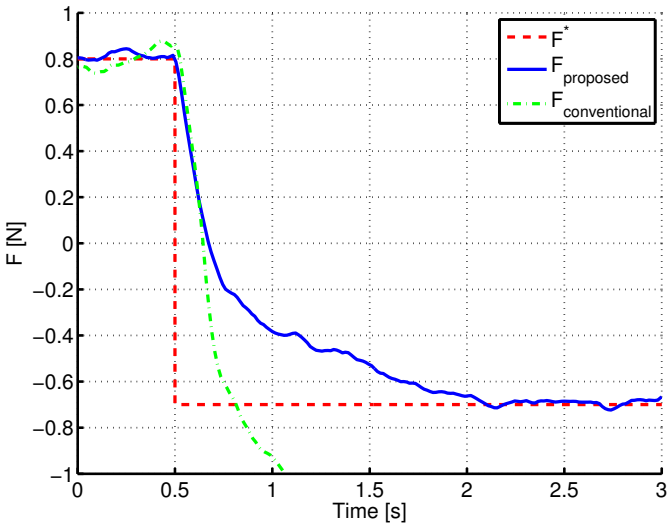

Fig. 8. Negative Step Responce

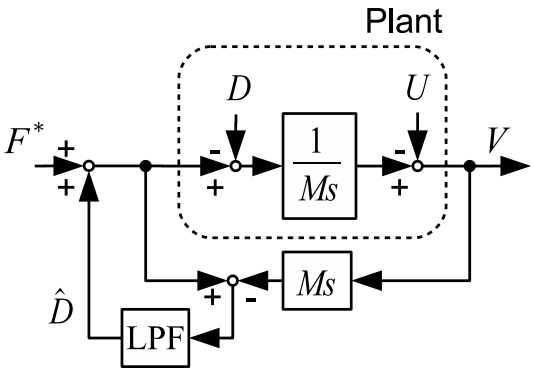

Fig. 9. Block Diagram Using Drag Observer

transfer function from F^* to F of the thrust controller is expressed as $G_F F^*$.

A. Designing of Drag Observer

The designing of drag observer is explained in this section. From Eq. (9) and Eq. (11), Drag D can be expressed as Eq. (21) when tailwind U is neglected.

$$D = F - M\dot{V} \tag{21}$$

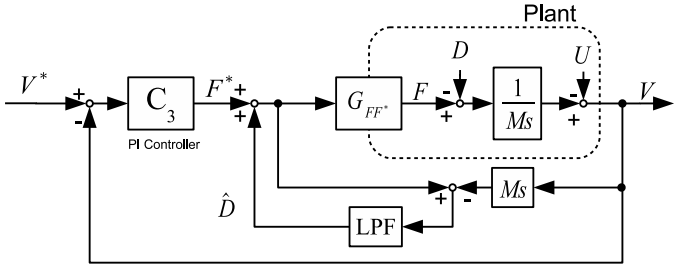

Fig. 10. Airspeed Controller

TABLE II. PARAMETERS OF FPEV2-KANON

Vehicle Mass (M_d)	860 [kg]
Vehicle Hight (H)	1.5 [m]
Vehicle Length (L)	2.9 [m]
Wheel Base (l)	1.7 [m]
Vehicle Width (W)	1.5 [m]
Front Wheel Inertia Moment (J_f)	1.24 [kg · m^2]
Front Wheel Inertia Moment (J_r)	1.26 [kg · m^2]
Wheel Radius (R_d)	0.302 [m]
Hight of Center of Gravity (h_g)	0.51 [m]

Estimated drag $\hat{D}$ can be obtained as Eq. (22) by using nominal mass of airplane M_n and Eq. (21).

$$\hat{D} = \frac{\omega_{\mathrm{DO}}}{s + \omega_{\mathrm{DO}}} \left(F^* - M_n \dot{V} \right) \tag{22}$$

This is called drag observer (DO). Here, the thrust controller is assumed to be sufficiently fast to suppose $F^* = F$.

The controller including the DO is shown in Fig. 9. In Fig. 9, the plant is nominalized by adding estimated drag $\hat{D}$ to thrust reference F^* in advance. Airspeed V can be expressed as Eq. (23), so in frequencies below cutoff frequency of the low pass filter, drag D and tailwind U is repressed, making the plant nominalized as 式 (24).

$$V = \frac{F^*}{M_n s} - D \frac{s\omega_{\mathrm{DO}}}{s + \omega_{\mathrm{DO}}} \frac{1}{M_n s} - U \frac{s\omega_{\mathrm{DO}}}{s + \omega_{\mathrm{DO}}} \tag{23}$$

$$V = \frac{F^*}{M_n s} \tag{24}$$

B. Designing of Airspeed Controller

In this section, airspeed controller is proposed. The airspeed controller is shown in Fig. 10.

Airspeed controller uses proportional-integral control. The gain is determined by pole placement method. The plant is assumed to be the nominal plant expressed by Eq. (24), and the pole was placed at $-\omega_3$.

VII. PROPOSAL OF NEW TOWING TEST METHOD

There are generally three main test methods to take aerodynamic performances. The first is by real flight, second by wind tunnel, and third by towing test. The only way to take transient response accompanying airspeed change is by real flight. However, experiment by real flight has many drawbacks. Real flight experimental unit must have the ability to fly. Namely, the unit must be light enough, have aerodynamic stability, have standard steering gears, etc. Because real flight has 6 degrees of freedom, interference between elemental technologies are unavoidable.

In this section, novel testing method called the infinite guide method is proposed. This method is a type of towing test, so the unit may not have the ability to fly. The degree of freedom is restricted, so only desired data can be examined.

A. Experimental Setup

An electric vehicle, FPEV2-Kanon shown in 図 11, is used for this towing test. The parameters of FPEV2-Kanon is shown in Table II.

Fig. 11. FPEV2–Kanon

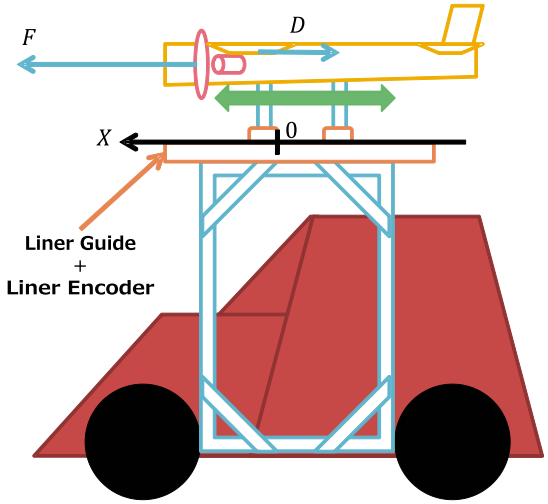

Fig. 12. Towing Experiment

B. Infinite Guide Method

The test unit is constrained on to a guide block with the guide rail fixed on to the EV. When the the test unit moves, the EV also moves so that the test unit stays within the range of the guide. This proposed method is called the infinite guide method.

In this paper, the towing test of the airspeed controller is done so that the test unit moves freely in the forward direction by a liner guide. The relative displacement is measured by a liner encoder. A controller that keeps the displacement of the EV and test unit X_r to 0 is designed. The controller for the electric vehicle for the infinite guide method is shown in Fig. 13. The upper half of the block diagram shows the airspeed controller of the test unit, and the lower half shows the controller of the electric vehicle which is proposed in this section. The friction is assumed to be very small. The test unit is not effected by the movement of the electric vehicle.

The controller of the EV has a speed controller in the inner loop and a relative displacement controller in the outer loop. The outer loop is not fast enough, so there is a feed forward speed reference generated from the airspeed controller of the test unit.

The wheel torque reference of the EV T_d^* is generated by $T_d^* = F_d^* R_d$ where F_d^* is the driving force reference.

First, the feedback speed controller of the EV C_{Vd} is explained. The equation of motion of the EV is as Eq. (25)

$$M_d \dot{V}_d = F_d \tag{25}$$

Here, the driving resistance is neglected. A proportional controller was used for the EV's speed controller. The gain was decided by the pole placement method, and the pole was placed at $-\omega_{Vd}$.

Next, the feed forward speed reference generator C_{VVd} is explained. Define G_{VV^*} as the transfer function from test unit's airspeed reference to the airspeed. Define G_{VdVd^*} as the transfer function from the EV's speed reference to the speed. G_{VV^*} and G_{VdVd^*} can be expressed as below using pole of test unit's airspeed controller $-\omega_3$ and pole of EV's speed controller ω_{Vd}.

$$G_{VV^*} = \frac{\omega_3}{s+\omega_3} \tag{26}$$

$$G_{VdVd^*} = \frac{\omega_{Vd}}{s+\omega_{V_d}} \tag{27}$$

The transfer function of C_{VVd} H_{VVd} is designed as Eq. (28). Than, the transfer function from V^* to V_d G_{VVd^*} can be written as Eq. (29). If there are no plant modeling error and and no disturbance, the EV's speed will follow the test unit's speed completely.

$$H_{VVd} = G_{VV^*} G_{VdVd^*}^{-1} \tag{28}$$

$$G_{VV_d^*} = G_{VV^*} \tag{29}$$

However, the actual situation has plant modeling error and disturbance, so feedback relative displacement controller C_{Xr} is designed. Proportional controller was used for C_{Xr}. Pole placement method is used to decide the gain. The plant is assumed to be $\frac{1}{s}$, and the pole is placed at $-\omega_{Xr}$.

C. Verification of Infinite Guide Method through Simulation

The poles of the speed controller $-\omega_{V_d}$ and ralative displacement controller $-\omega_{Xr}$ were placed at -50 rad/s, and -5 rad/s respectively.

Simulation was taken in place so that the airspeed reference for the test unit was given as a step reference from 7 m/s to 8 m/s. Simulation results are shown in Fig. 14(a) and Fig. 14(b). Fig. 14(a) shows the speed of the test unit and EV. Fig. 14(b) shows the relative displacement. The relative displacement is within $\pm$10cm.

VIII. Conclusion

In this paper, a new thrust control method of a single propeller electric airplane for higher maneuverability was proposed. First, the single propeller electric airplane was modeled. Next, a thrust control method with a revolution speed control in the inner loop was proposed based on the proposed model. Finally, simulation and experiment was carried out, and the proposed method was verified to have quick and

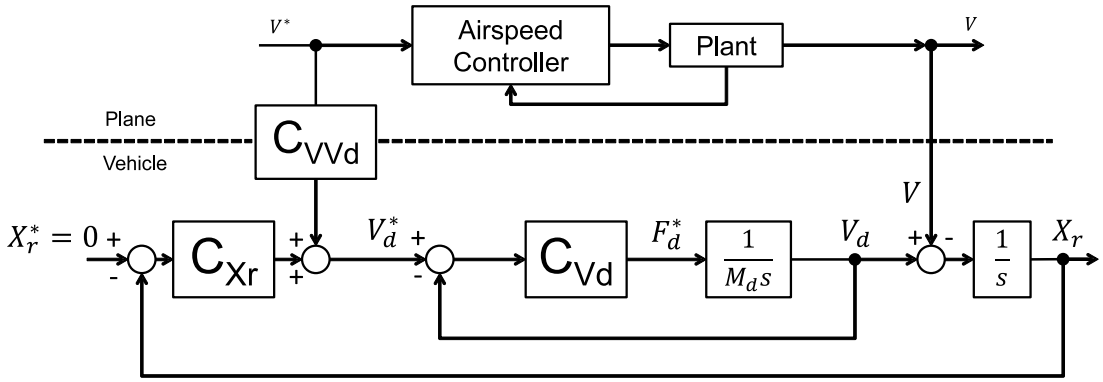

Fig. 13. Infinate Guide Method

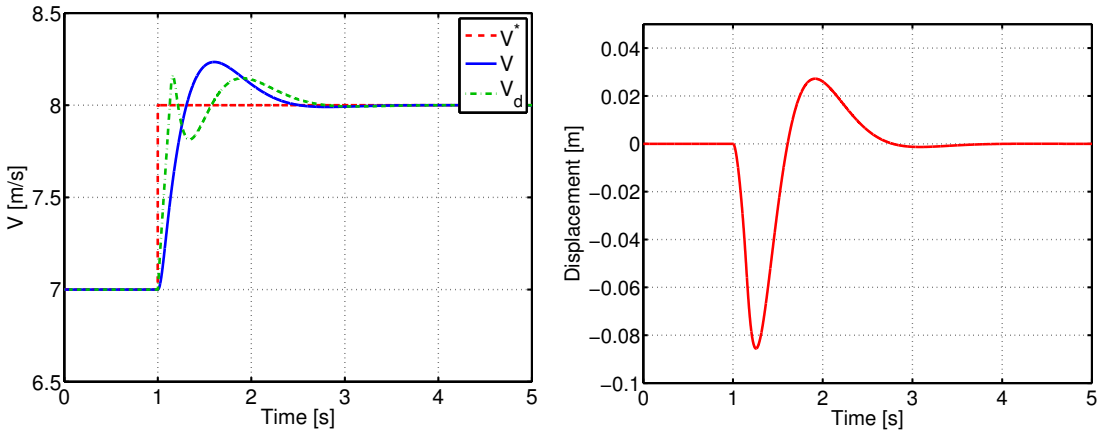

(a) Velocity

(b) Displacement

Fig. 14. Simulation Results for Towing Experiment

accurate response to the reference, and has high robustness to disturbance.

A airspeed control method was omitted from this paper due to limitations of space, but is published and read at 51th AIRCRAFT SYMPOSIUM hosted by JSASS [13].

References

[1] Michael P. Huerta: "FAA Aerospace Forecast Fiscal Years 2012-2032," FAA Aerospace Forecast Fiscal Years 2012-2032, (2012).

[2] International Business Aviation Council: "Business aviation safety brief," International Business Aviation Council, No. 10 (2011-9).

[3] Aviation Safety: "Statistical Summary of Commercial Jet Airplane Accidents," Statistical summery, Boeing Commercial Airplanes (2011-6).

[4] R. Kebabjian: "Accident Statistics". PlaneCrashInfo.com (2010).

[5] "The 2011 Green Flight Challenge Sponsored by Google," CAFE Foundation. CAFE Foundation, Web. (2012).

[6] K. Nam, Y. Kim S. Oh, and Y. Hori: , "Steering Angle-Disturbance Observer (SA-DOB) based yaw stability control for electric vehicles with in-wheel motors," Control Automation and Systems (ICCAS), 2010 International Conference on , vol., no., pp.1303-1307 (2010-10).

[7] Y. Chen, J. Wang; "Energy-efficient control allocation with applications on planar motion control of electric ground vehicles," American Control Conference (ACC), 2011, pp.2719-2724 (2011-6).

[8] Venkatesh Prasad, K.; Broy, M.; Krueger, I., "Scanning Advances in Aerospace & Automobile Software Technology," Proceedings of the IEEE , vol.98, no.4, pp.510,514 (2010-4).

[9] A. Nishizawa, H. Kobayashi, K. Okai, and H. Fujimoto: "Progress of Electric Vehicle Technology and Future of Electric Aircraft," The 43rd JSASS Annual Meeting, pp. 521–526 (2012) (in Japanese).

[10] T. Tucker: "Touchdown: The Development of Propulsion Controlled Aircraft at NASA Dryden," Monographs in Aerospace History, No. 16, Washington (1999).

[11] Kenichiro Takahashi, Hiroshi Fujimoto, Yoichi Hori, Hiroshi Kobayashi, Akira Nishizawa, Modeling of Propeller Electric Airplane and Thrust Control using Advantage of Electric Motor, The 13th International Workshop on Advanced Motion Control, pp. 482-487 (2014).

[12] Karl Falk: "Aircraft PRopeller Handbook," The Ronald Press Company, New York (1937).

[13] Kenichiro Takahashi, Hiroshi Fujimoto, Yoichi Hori, Hiroshi Kobayashi, Akira Nishizawa, "Control of Electric Airplane's Airspeed using Advantage of Electric Motor and Proposal of Test Method with Electric Vehicle", 51th AIRCRAFT SYMPOSIUM (2013) (in Japanese).